

## **Photoluminescence, Scanning Electron Microscope and Atomic Force Microscope Analyses of Organic NLO Single Crystal of Hippuric Acid for Opto-electronic and Photonic Applications**

**N. Mahalakshmi, M. Parthasarathy\***

Department of Physics, School of Basic Sciences, Vels Institute of Science, Technology and Advanced Studies, Pallavaram, Chennai-600 117, Tamilnadu, India

Received 6 July 2023, accepted in final revised form 13 November 2023

### **Abstract**

A bulk single crystal of Hippuric acid (HA) was grown by a low temperature solution growth technique. The unit cell parameters were confirmed by single crystal X-ray diffraction. The optical transmittance of grown crystal was determined by UV-Vis-NIR analysis and the lower cut-off wavelength was observed at 304 nm. The Urbach energy shows HA has good crystallinity. Photoluminescence study reveals the suitability of the grown crystal for near- violet fluorescence emission. The electronic polarizability was calculated by using Lorentz-Lorenz equation. Scanning Electron Microscope (SEM) analysis, reveals that the material surface is like layer structure. Atomic Force Microscope (AFM) analysis was used to analyse the surface roughness of the grown material.

*Keywords:* Single crystal growth; Urbach energy; Electronic polarizability; Photoluminescence.

© 2024 JSR Publications. ISSN: 2070-0237 (Print); 2070-0245 (Online). All rights reserved.  
doi: <https://dx.doi.org/10.3329/jsr.v16i2.67430> J. Sci. Res. **16** (2), 449-457 (2024)

### **1. Introduction**

The demand for ultrafast effective information transmission processing increases with an increase in the amount of information that society deals with. Electronic and photonic materials are the key elements of continued scientific growth and technological advances in the new millennium. The non-linear optical (NLO) properties of large organic molecules have been subjected to extensive theoretical and experimental investigations during the past two decades for generating the second harmonic frequency plays an important role in the domain of optoelectronics and photonics [1]. Nonlinear optical materials are used in abundance for Telecommunications, Electro-Optic Modulators, High-Density Optical Memories, Optical Bistability, Color Displays, etc. [2]. NLO organic materials were targeted due to their NLO efficiency satisfies the optical applications. On compared with other materials, mixed crystals of organic with amino acid shows great NLO behaviour [3]. In comparison to inorganic materials, the organic NLO

---

\*Corresponding author: [mps2k7@gmail.com](mailto:mps2k7@gmail.com)

crystals get more attention, because these crystals have very high (SHG and THG) optical susceptibilities and intrinsically rapid response times [4]. Hippuric acid is one of the organic nonlinear optical materials having second harmonic generation. The second harmonic generation behavior and NLO properties and density functional theoretical study of HA crystal was studied by several researchers [5-7]. We have reported the growth methodology and some of the characterizations like CHN, FT-IR, UV-Vis absorbance, Second Harmonic Generation, Laser Damage Threshold, and Antibacterial activity [8]. In the present work, we attempt new studies such as estimation of Urbach energy, optical constants, electronic polarizability and photoluminescence. Scanning Electron Microscope (SEM) and Atomic Force Microscope (AFM) analyses were also used.

## 2. Experimental

The low-temperature solution growth technique was widely used for the growth of organic and inorganic compounds to get good-quality single crystals. Hippuric acid (HA) is a white crystalline powder that has a molecular formula  $C_9H_9NO_3$  with a molecular weight of 179.18 g/mol. The analytical grade HA was taken and dissolved in Dimethyl formamide to prepare the saturated solution. The saturated solution of HA was obtained by dissolving the material with continuous stirring of the solution using a magnetic stirrer. The resulting solution was filtered with Whatman filter paper. The filtered solution was allowed to evaporate in a beaker at ambient temperature. Optically transparent bulk single size of  $15 \times 4 \times 3 \text{ mm}^3$  was harvested in 25 days. The as-grown single crystal is displayed in Fig. 1.

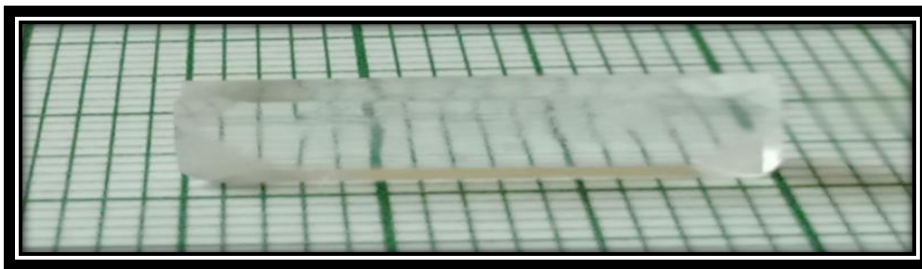


Fig. 1. As grown single crystal of HA.

## 3. Results and Discussion

### 3.1. Single crystal XRD analysis

The single crystal X-ray diffraction analysis enumerates that the title compound belongs to the orthorhombic crystal system with space group  $P2_12_12_1$ . The observed lattice cell parameter values are  $a = 8.787 (4) \text{ \AA}$ ,  $b = 10.592 (4) \text{ \AA}$ ,  $c = 9.096 (4) \text{ \AA}$ ,  $\alpha = \beta = \gamma = 90^\circ$  and volume  $846 \text{ \AA}^3$ , matched with the reported literature values [9].

### 3.2. Optical studies

Transparent HA crystal was analyzed in the range of 200-1100 and the sample of about 1 mm thickness was taken for UV-Vis-NIR study. Fig. 2 shows UV-Vis-NIR transmittance image of HA. It shows the good transparency in the entire visible region.

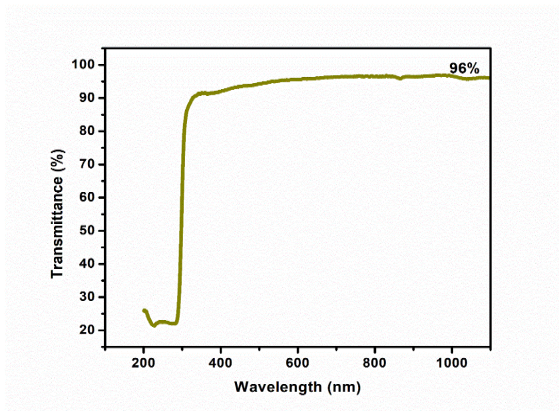


Fig. 2. UV-Vis-NIR transmittance image of HA.

Lower cut-off wavelength of the material was found to be 304 nm. The optical absorption coefficient ( $\alpha$ ) is calculated using “Eq. (1)” as follows,

$$\alpha = \frac{2.3026}{t} \log \frac{1}{T} \tag{1}$$

The dependence of the optical absorption coefficient ( $\alpha$ ) with the photon energy helps to study the band structure, where  $\alpha$  is the absorption coefficient,  $h\nu$  is photon energy,  $E_g$  is the optical band gap energy,  $A$  is a constant and  $m$  is the optical transition number. When electromagnetic radiation is passed into the materials, it is absorbed at a certain wavelength when the energy equals the optical band gap energy of the materials. Electron transition between the valence and conduction bands can be direct or indirect and possess forbidden transition [10]. The transition number ( $m$ ) is  $1/2$ ,  $2$ ,  $3/2$ , and  $3$  for the direct allowed transition, indirect allowed transition, direct forbidden transition, and indirect forbidden transition respectively [11].  $E_g$  was assessed using “Eq. (2)”

$$\alpha h\nu = A(E_g - h\nu)^m \tag{2}$$

Fig. 3 shows band gap energy of the grown material. The band gap was found as 4.07 eV.

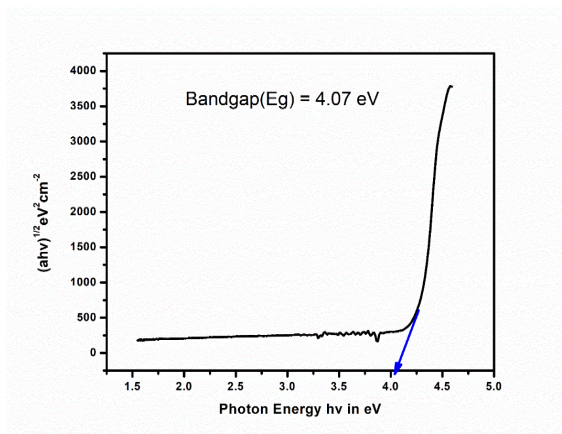


Fig. 3. Variation of photon energy ( $h\nu$ ) with  $(\alpha h\nu)^{1/2}$ .

### 3.3. Absorption band tail (Urbach energy)

The relationship between  $\alpha$  and energy of photons ( $h\nu$ ) is known as Urbach empirical rule [12,13], which is given by the following exponential “Eq. (3)”

$$\alpha = \alpha_0 \exp\left(\frac{h\nu}{E_U}\right) \quad (3)$$

where  $\alpha_0$  is a constant and  $E_U$  denotes the energy of the band tail or sometimes called Urbach energy [14]. Taking the logarithm on both sides of “Eq. (3)”, one can get an equation of straight line and it is given as follows: “Eq. (4)”

$$\ln(\alpha) = \ln(\alpha_0) + \left(\frac{h\nu}{E_U}\right) \quad (4)$$

Urbach energy ( $E_U$ ) obtained from the reciprocal of the slope of the straight line obtained by plotting  $\ln(\alpha)$  vs  $h\nu$ . Which value was found to be 0.133 eV, which is shown in Fig. 4.

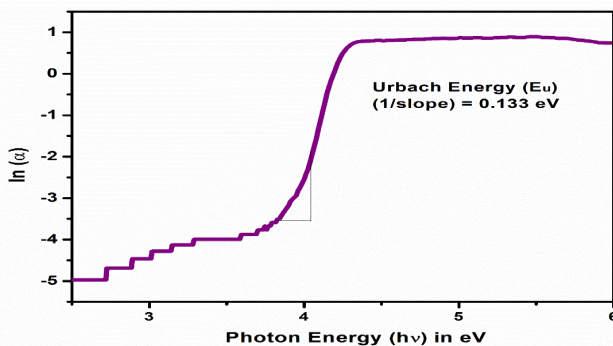


Fig. 4. Plot of  $\ln(\alpha)$  against photon energy ( $h\nu$ ).

The steepness parameter ( $\sigma$ ) was evaluated from “Eq. (5)”

$$\sigma = \frac{K_B T}{E_U} \tag{5}$$

The value of  $\sigma$  was 0.176, which is used for relating the strength of the electron-phonon interaction [15,16] ( $E_{e-p}$ ), calculated by “Eq. (6)”

$$E_{e-p} = \frac{2}{3\sigma} \tag{6}$$

Electron-phonon interaction energy ( $E_{e-p}$ ) was found to be 3.78. The detailed parameters values are given in Table 1.

Table 1. Urbach Energy of HA single crystal.

Description	Value
Cut-off wavelength (nm)	304 nm
Optical bandgap $E_g$	4.07 eV
Urbach energy $E_U$	0.133 eV
Steepness parameter $\sigma$	0.176
$E_{e-p}$	3.78

### 3.4. Evaluation of optical parameters

Extinction coefficient (K) is calculated by “Eq. (7)”. The extinction coefficient vs photon energy is shown in Fig. 5.

$$K = \frac{\alpha\lambda}{4\pi} \tag{7}$$

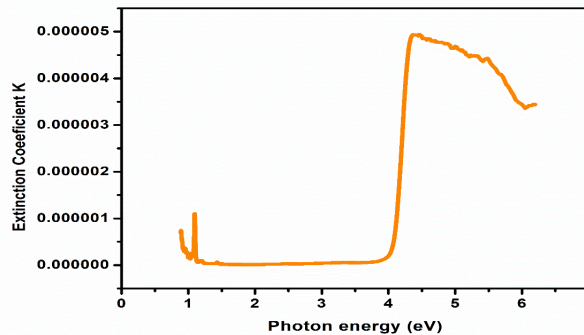


Fig. 5. Plot of photon energy against extinction coefficient.

The refractive index (n) was estimated by using “Eq. (8)”

$$n = \frac{-(R+1) \pm \sqrt{(-3R^2+10R-3)}}{2(R-1)} \tag{8}$$

The spectrum of refractive index ( $n_0$ ) vs Wavelength ( $\lambda$ ) is shown in Fig. 6.

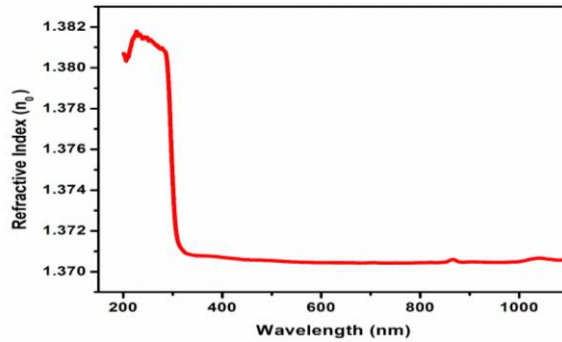


Fig. 6. Wavelength dependence of refractive indices ( $n_0$ ).

From the spectrum, the linear refractive index was 1.37 at 532nm. The optical conductivity ( $\sigma_{op}$ ) is a measure of the frequency response of the material when irradiated by light and it was calculated by using “Eq. (9)”.

Fig. 7 displays the optical conductivity vs photon energy of the grown crystal.

$$\sigma_{op} = \frac{anc}{4\pi} \quad (9)$$

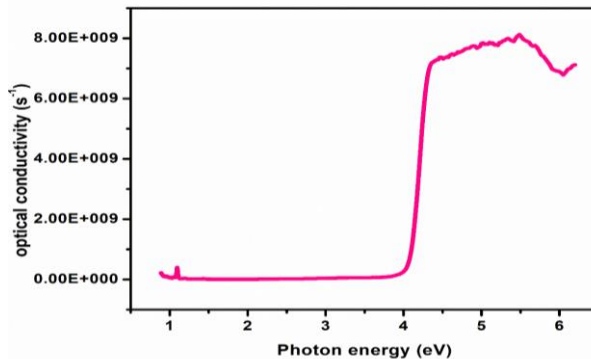


Fig. 7. Optical conductivity as a function of photon energy.

HA shows a high magnitude of optical conductivity confirming the presence of a very high photo response nature of the title crystal for device fabrication.

### 3.5. *Electronic polarizability ( $\alpha$ )*

The parameter of electronic polarizability ( $\alpha$ ) [17] is calculated using “Eq. (10)” [18] and the value is  $2.2382 \times 10^{-23} \text{ cm}^3$ .

$$\alpha = \frac{3M}{\pi N_A \rho} \left[ \frac{n_0^2 - 1}{n_0^2 + 2} \right] \text{ cm}^3 \quad (10)$$



### 3.6. Photoluminescence (PL) studies

Photoluminescence is a non-destructive method of study the electronic structure of materials [19]. The PL intensity is highly dependent on the crystallinity and structural perfection excitation wavelength of 290 nm was applied, and a sharp peak was observed in the range of 300-350 nm in the emission spectrum peaking at 306 nm shown if Fig. 8 (high intensity peak 1498906 a.u.), which results in usage in optoelectronic devices [20] and suitability is for near-violet fluorescence emission.

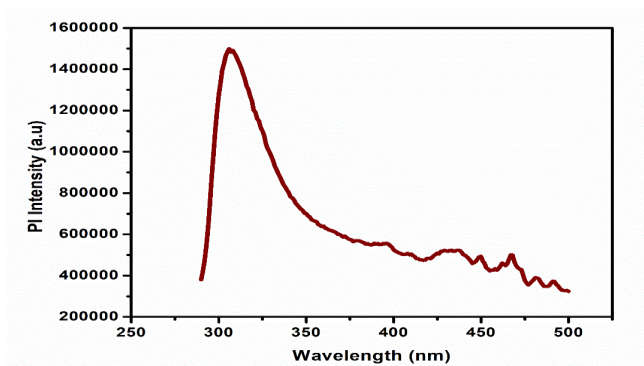


Fig. 8. Photoluminescence spectrum of HA.

### 3.7. Scanning Electron Microscope (SEM) Analysis

The SEM micrographs of HA were taken at room temperature with magnification ranges 800 and 2000 in the operating voltage of 20 kV are listed in Figs. 9(a) and 9(b)., it indicates the growth needle layer pattern of the HA, which is shown in Fig. 9(a).

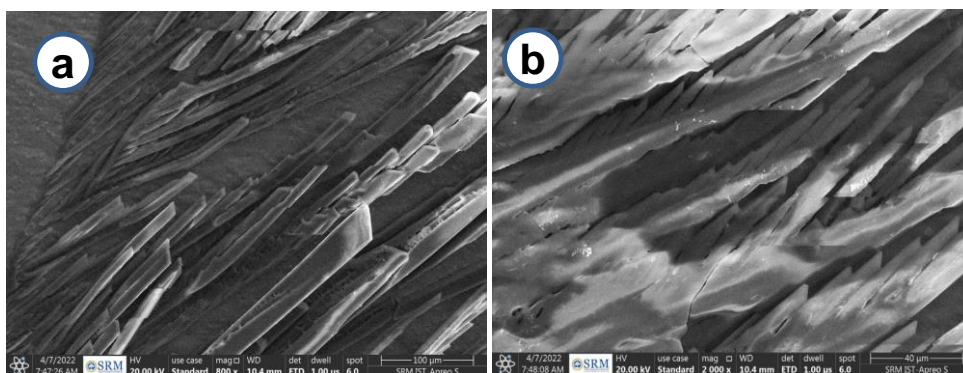


Fig. 9. SEM micrographs of HA single crystal in different magnification scales.

### 3.8. Atomic force microscope (AFM) analysis

AFM topographical images of Hippuric acid single crystals 3D and 2D images are in Figs. 10(a) and 10(b). In an AFM, the mechanical interaction between the tip and the material is exploited to yield surface topography. Bulges are found in upper face of the crystal clearly indicating radiation-induced sputtering as well as amorphization on its surface. The hillocks dimensions formed after irradiation are also shown in the AFM images.

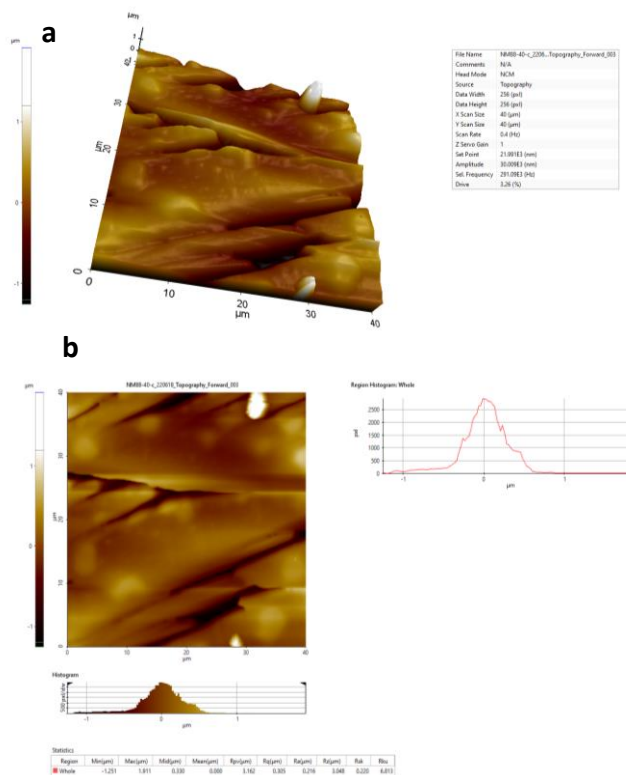


Fig. 10. AFM images of HA: a) 3D and b) 2D.

## 4. Conclusion

Low temperature solution growth technique was used to grow optically transparent bulk crystal at room temperature. Single XRD reveals the crystal structure. UV-Vis- NIR analysis showed that cut off wavelength is 304 nm and a band gap is 4.07 eV. Urbach energy ( $E_U$ ) is 0.133 eV, shows good crystallinity of the grown crystal. PL confirmed the material is suitable for near-violet fluorescence emission. SEM image analysis with 40  $\mu\text{m}$  and 100  $\mu\text{m}$  scale revealed the needle shape on the surface of grown micro crystals. AFM analysis is a three-dimensional topographic technique with a high atomic resolution was used to measure surface roughness of grown crystal.



## Acknowledgment

We greatly acknowledged SAIF, IIT-Madras, Chennai – 600 036 for the data collection of single crystal from XRD. The authors also extend their gratitude and acknowledge to Vels Institute of Science, Technology and Advanced Studies, Pallavaram, Chennai-600 117, Tamilnadu, India for AFM studies. The authors extend their acknowledgment to B. S. Abdur Rahman Crescent Institute of Science & Technology, Chennai - 600 048 for UV-Vis-NIR analysis and photoluminescence studies.

## References

1. M. N. Bhat and S. M. Dharmaprasanna, J. Cryst. Growth **243**, 526 (2002). [https://doi.org/10.1016/S0022-0248\(02\)01446-X](https://doi.org/10.1016/S0022-0248(02)01446-X)
2. K. Selvaraju, R. Valluvan, and S. Kumararaman, Mater. Lett. **60**, 1549 (2006). <https://doi.org/10.1016/j.matlet.2005.11.100>
3. B. Ravindran, R. S. A. shiny, T. L. B. Beno, and N. Lavanya, Mater. Today: Proc. **80**, 3634 (2023). <https://doi.org/10.1016/j.matpr.2021.07.340>
4. B. S. I. Lasalle, M. S. Pandian, K. Anitha, and P. Ramasamy, Inorg. Chem. Commun. **157**, ID 111397 (2023). <https://doi.org/10.1016/j.inoche.2023.111397>
5. N. Vijayan, R. R. Babu, R. Gopalakrishnan, P. Ramasamy, M. Ichimura, and M. Palanichamy, J. Cryst. Growth **273**, 564 (2005). <https://doi.org/10.1016/j.jcrysgro.2004.09.058>
6. N. Vijayan, G. Bhagavannarayana, and A. M. Z. Slawin, Mater. Lett. **62**, 2480 (2008). <https://doi.org/10.1016/j.matlet.2007.12.053>
7. M. Karabacak, M. Cinar, and M. Kurt, Spectrochim Acta Part A **74**, 1197 (2009). <https://doi.org/10.1016/j.saa.2009.09.035>
8. N. Mahalakshmi and M. Parthasarathy, J. Neuro Quantol. **20**, 6779 (2022).
9. H. Ringertz, Acta Cryst. **B27**, 285 (1971). <https://doi.org/10.1107/S0567740871002115>
10. N. Chopra, A. Mansingh, and G. K. Chadha, J. Non-Cryst. Solids **126**, 194 (1990). [https://doi.org/10.1016/0022-3093\(90\)90819-8](https://doi.org/10.1016/0022-3093(90)90819-8)
11. J. Melsheimer, D. Ziegler, Thin Solid Films **129**, 35 (1985). [https://doi.org/10.1016/0040-6090\(85\)90092-6](https://doi.org/10.1016/0040-6090(85)90092-6)
12. S. J. Ikhmayies and R. N. Ahmad-Bitar, J. Mater. Res. Technol. **2**, 221 (2013). <https://doi.org/10.1016/j.jmrt.2013.02.012>
13. K. A. Aly, A. M. A. Elnaeim, M. A. M. Uosif, and O. Abdel-Rahim, Physica B: Condensed Matter **406**, 4227 (2011). <https://doi.org/10.1016/j.physb.2011.08.013>
14. F. Urbach, Phys. Rev. **92**, 1324 (1953). <https://doi.org/10.1103/PhysRev.92.1324>
15. M. Karimi, M. Rabiee, F. Moztafzadeh, M. Tahriri, and M. Bodaghi, Curr. Appl. Phys. **9**, 1263 (2009). <https://doi.org/10.1016/j.cap.2009.02.006>
16. R. Hanumantharao, S. Kalainathan, and G. Bhagavannarayana, Spectrochim Acta Part A **91**, 345 (2012). <https://doi.org/10.1016/j.saa.2012.02.023>
17. N. M. Ravindra and V. K. Srivastava, J. Infrared Phys. **20**, 67 (1980). [https://doi.org/10.1016/0020-0891\(80\)90009-3](https://doi.org/10.1016/0020-0891(80)90009-3)
18. P. Karuppasamy, V. Sivasubramani, M. S. Pandian, and P. Ramasamy, RSC Adv. **6**, 109105 (2016). <https://doi.org/10.1039/C6RA21590D>
19. O. Mondal, J. Sci. Res. **14**, 831 (2022). <https://doi.org/10.3329/jsr.v14i3.58384>
20. J. X Wang, S. S Xie, H. J. Yuan, X. Q. Yan, D. F. Liu, Y. Gao, Z. P. Zhou, L. F. Liu, X. W. Zhou, X. Y. Dou, W. Y. Zhou, and G. Wang, Solid State Commun. **131**, 435 (2004). <https://doi.org/10.1016/j.ssc.2004.06.009>